Surface Climate Variations over the North Atlantic Ocean during Winter: 1900–1989

CLARA DESER

Cooperative Institute for Research in Environmental Sciences, University of Colorado, Boulder, Colorado

MAURICE L. BLACKMON

Climate Research Division, NOAA/Climate Monitoring and Diagnostics Laboratory, Boulder, Colorado

(Manuscript received 9 October 1992, in final form 17 March 1993)

ABSTRACT

The low-frequency variability of the surface climate over the North Atlantic during winter is described, using 90 years of weather observations from the Comprehensive Ocean–Atmosphere Data Set. Results are based on empirical orthogonal function analysis of four components of the climate system: sea surface temperature (SST), air temperature, wind, and sea level pressure. An important mode of variability of the wintertime surface climate over the North Atlantic during this century is characterized by a dipole pattern in SSTs and surface air temperatures, with anomalies of one sign east of Newfoundland, and anomalies of the opposite polarity off the southeast coast of the United States. Wind fluctuations occur locally over the regions of large surface temperature anomalies, with stronger-than-normal winds overlying cooler-than-normal SSTs. This mode exhibits variability on quasi-decadal and biennial time scales. The decadal fluctuations are irregular in length, averaging ~9 years before 1945 and ~12 years afterward. There does not appear to be any difference between the wind–SST relationships on the different time scales. The decadal fluctuations in SSTs east of Newfoundland are closely linked to decadal variations in sea ice in the Labrador Sea, with periods of greater than normal sea ice extent preceding by ~2 years periods of colder-than-normal SSTs east of Newfoundland.

Another dominant mode of variability is associated with the global surface warming trend during the 1920s and 1930s. The patterns of SST and air temperature change between 1900–29 and 1939–68 indicate that the warming was concentrated along the Gulf Stream east of Cape Hatteras. Warming also occurred over the Greenland Sea and the eastern subtropical Atlantic. The warming trend was accompanied by a decrease in the strength of the basin-scale atmospheric circulation (negative phase of the North Atlantic Oscillation). In marked contrast to the dipole pattern, the wind changes occurred downstream of the largest SST anomalies; hence, the gradual surface warming along the Gulf Stream may have been a result of altered ocean currents rather than local wind forcing.

1. Introduction

Climate variability on decadal and longer time scales is a subject of increasing interest and relevance. With concern over anthropogenic effects on global climate, there is a strong impetus to describe and understand the natural modes of variability of the climate system. In this study, we focus on the low-frequency climate fluctuations over the North Atlantic Ocean since the turn of the century.

The North Atlantic is a region of particular importance to the global climate system. The formation of bottom water at high latitudes of the North Atlantic drives a transequatorial thermohaline circulation. Changes in the rate of deep-water production (and, hence, in the strength of the thermohaline circulation) can have a profound effect on global climate, as inferred from paleoclimate data (Broeker et al. 1986; Lehman and Keigwin 1992) and as shown by the modeling studies of Rind et al. (1986) and Manabe and Stouffer (1988). Recent ocean modeling experiments indicate that self-sustained oscillations of the thermohaline circulation can occur on decadal and longer time scales (Weaver and Sarachik 1991).

Low-frequency climate fluctuations in the North Atlantic since World War II have been investigated in several studies. Levitus (1989) used subsurface measurements of temperature and salinity to document a major shift in the ocean circulation in the North Atlantic between the late 1950s and the early 1970s. Knox et al. (1988) showed that the Northern Hemisphere atmospheric circulation experienced an abrupt transition during the early 1960s (see also Flohn 1986 and Shabbar et al. 1990). One of the best documented examples of low-frequency variability at high latitudes of the North Atlantic is the "Great Salinity Anomaly," a freshwater mass that was observed to travel around the subpolar gyre during 1968–82 (Dickson et al. 1988).

Corresponding author address: Dr. Clara Deser, CIRES, Campus Box 449, University of Colorado, Boulder, CO 80309-0449.

The freshening of the surface waters was sufficient to temporarily halt deep water formation in the Labrador Sea (Lazier 1988). Mysak et al. (1990) discuss the relationship between the great salinity anomaly and the Arctic climate system.

Studies dealing with the longer (100 yr) marine records have tended to emphasize globally averaged surface temperature variations (cf. Paltridge and Woodruff 1981; Jones and Kelly 1983; Barnett 1984; Folland et al. 1984; Jones et al. 1986). These studies find that the dominant signal in worldwide temperatures is a warming trend during ~1920–40, with the largest amplitudes at high latitudes.

Bjerknes (1959, 1961, 1962, 1964) investigated air–sea interaction in the North Atlantic on time scales ranging from interannual to interdecadal. Using data from 1890 to 1940, Bjerknes provided compelling evidence that interannual fluctuations in SST are largely governed by wind-induced changes in latent and sensible heat fluxes at the sea surface. However, the long warming trend during the first quarter of this century appears to be linked to a change in the ocean circulation rather than air–sea energy fluxes (Bjerknes 1959). Similar conclusions regarding interannual and interdecadal SST variations are reached by Kushnir (1992).

The purpose of this study is to describe the variability of the winter climate over the North Atlantic Ocean using 90 years of surface marine data. The North Atlantic is the only ocean basin with sufficiently dense data coverage for a regional study of climate change since 1900. We focus on the winter season because 1) the atmosphere–ocean coupling is vigorous, and 2) the SST variations reflect significant changes in upper-ocean heat content. We are particularly interested in whether the climate system exhibits preferred time scales of variability, and whether the atmosphere–ocean relationships change with frequency. Our results are based on an objective (empirical orthogonal function) analysis of four components of the climate system: SST, air temperature, wind, and sea level pressure. We will show that the surface climate over the North Atlantic exhibits coherent decadal fluctuations that resemble the variations on interannual time scales. We will also show that the Gulf Stream may have been involved in the long-term warming trend during the 1920s and 1930s.

The data and methods are described in section 2. The two leading modes of surface temperature variability during 1900–89 and their relation to the atmospheric circulation are documented in section 3 and the results are discussed in section 4.

2. Data and methods

a. Data

The surface wind, sea level pressure, SST, and surface air temperature data used in this study are from the Comprehensive Ocean–Atmosphere Data Set (COADS), an extensive compilation of weather observations from merchant ships (see Woodruff et al. 1987). We have used data gridded by 4° latitude/longitude squares for the period 1900–1989. The COADS data are uncorrected for changes in instrumentation, observing practice, ship type, etc. Spurious trends resulting from these changes have been reported in surface wind speed and SST over the tropical oceans (Ramage 1987; Wright 1986; Cardone et al. 1990). Our approach to the issue of whether the routine ship-based measurements are sufficiently accurate and homogeneous to allow the detection of real climate signals is to demonstrate physical consistency among independent variables: wind patterns are compared to pressure distributions, and SST fields to surface air temperatures.

b. Methods

The monthly mean data were converted to anomalies by subtracting long-term monthly mean values for the period 1900–89. These monthly anomalies were then averaged into seasonal anomalies (November–March) to form winter-mean departures from normal. The winter-mean value was considered missing if two or more months in a winter were missing.

EOF analysis was used to identify objectively the dominant modes of variability in the North Atlantic climate system during the period 1900–89. EOF analysis was performed separately on the SST and air temperature fields. A combined EOF analysis was performed on the sea level pressure and zonal wind fields. EOFs were calculated using only those grid squares with at least 60 years of winter-averaged data. A minimum of 50 grid squares containing data in each winter was required to reconstruct the principal components (time series of the EOFs).

Linear regression analysis between the atmospheric parameters and the principal components of SST was used to define the circulation anomalies that accompany the SST variations.

3. Results

a. EOF modes of surface temperature variability

Figure 1 shows the first two EOFs of SST over the North Atlantic, superimposed upon the long-term mean SST distribution. The EOFs are based on unnormalized winter-mean (November–March) anomalies during the period 1900–89. The first EOF (Fig. 1a; hereafter referred to as E1 SST), which accounts for 45% of the variance, has uniform polarity over the entire basin. The largest loadings occur along the Gulf Stream (the latter is indicated by the tightly packed isotherms in the climatology). The time series of E1 SST (Fig. 1b) exhibits a sudden transition from below-normal values to above normal values around World War II. It is well known that the technique for measuring SSTs aboard ships changed during the early

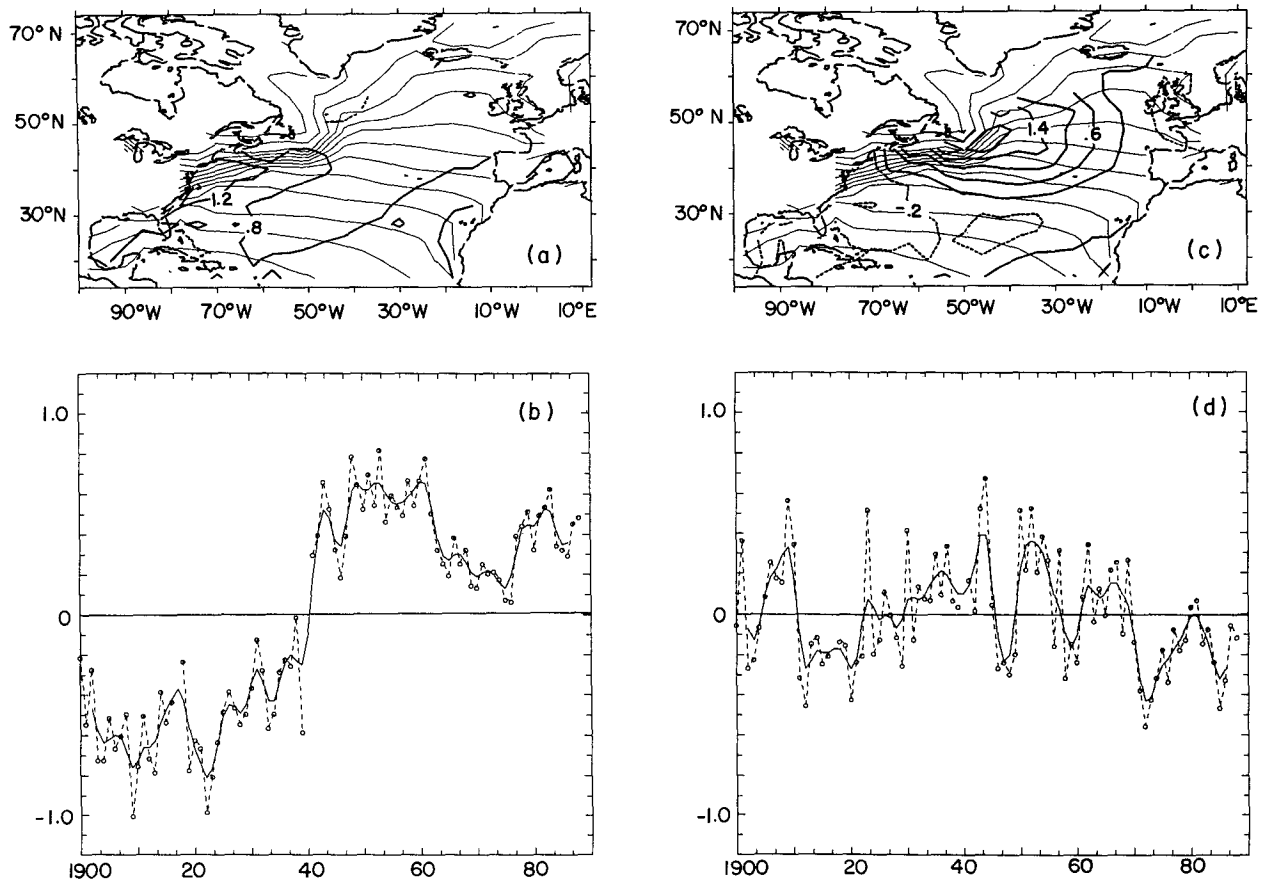

FIG. 1. (a) EOF 1 of North Atlantic SST anomalies based on unnormalized winter (November–March) means, 1900–1989 (bold contours). This mode accounts for 45% of the variance. Also shown is the climatological SST distribution (thin contours). (b) Time series of EOF 1 (dashed curve) and smoothed with a five-point binomial filter (solid curve). The circles denote the winter anomaly, plotted in the year in which November occurs. (c) As in (a) but for EOF 2. This mode accounts for 12% of the variance. (d) As in (b) but for EOF 2.

1940s, and that the bucket temperatures used before World War II were ~0.3°C lower than the engine intake samples used later (cf. Wright 1986; Folland et al. 1984). Over the Gulf Stream this difference can reach ~0.8°C, due to the rapid evaporative cooling from the bucket samples (Bottomley et al. 1990). Thus, one may be tempted to disregard E1 SST; however, air temperatures exhibit a similar EOF pattern with a more realistic time series (see below).

The second EOF (Fig. 1c), which accounts for 12% of the variance, exhibits a center of action east of Newfoundland at the boundary between the subtropical and subpolar ocean gyres. A weaker center of opposite polarity is located off the southeastern United States. The time series of E2 SST (Fig. 1d) exhibits quasi-biennial fluctuations (dashed curve) as well as quasi-decadal variations, particularily after ~1946 (solid curve). Longer-term trends are also evident.

The first two EOFs of air temperature, shown in Fig. 2, are similar to those of SST, but the order of the modes is reversed. The E1 of air temperature (Fig. 2a), which accounts for 21% of the variance, exhibits centers of action off Newfoundland and the southeastern United States; the correlation between the time series of E1 of air temperature and E2 of SST is 0.76.[1] The E2 of air temperature (Fig. 2c), which accounts for 17% of the variance, exhibits maximum amplitude along the Gulf Stream and near western Europe. The time series of E2 (Fig. 2d) is dominated by a long warming trend from the 1920s to the 1940s, followed by a cooling trend during the 1950s and 1960s. These trends follow those of global air temperature (Folland et al. 1984). Shorter-period fluctuations are also apparent.

The power spectra of E2 of SST and E1 of air temperature, based on the lag-correlation method, are shown in Fig. 3. The E1 of air temperature (bottom) exhibits spectral peaks at ~10–15 years and ~2–2.5

[1] All of the correlation coefficients cited in this study are statistically significant at the 99% level or higher, based on a one-tailed Student's t-test and taking into account the autocorrelation in the time series according to Leith (1973).

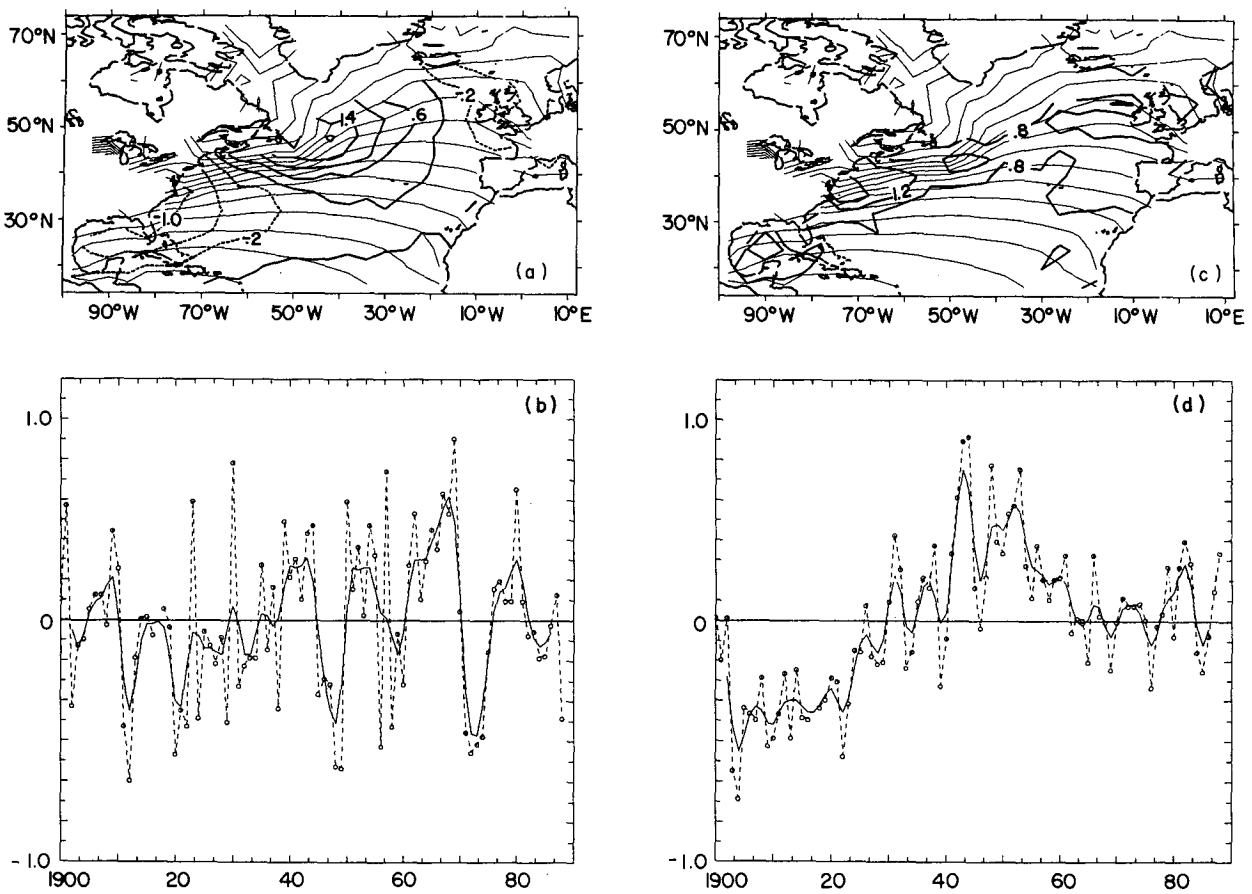

FIG. 2. (a) EOF 1 of North Atlantic surface air temperature anomalies based on unnormalized winter (November–March) means, 1900–1989 (bold contours). This mode accounts for 21% of the variance. Also shown is the climatological air temperature distribution (thin contours). (b) Time series of EOF 1 (dashed curve) and smoothed with a five-point binomial filter (solid curve). (c) As in (a) but for EOF 2. This mode accounts for 17% of the variance. (d) As in (b) but for EOF 2.

years, consistent with our visual impression of the time series. Both spectral peaks are statistically significant at the 95% level (a priori) above the red noise background. The power spectrum of E2 SST is red, with a suggestion of a peak at the decadal period, and a significant peak at the biennial period. The power spectra of E2 of air temperature and E1 of SST (not shown) are red, reflecting the dominance of the long trends before and after World War II.

We have examined the sensitivity of the leading EOF patterns of air temperature to temporal filtering. In view of the power spectrum of E1 of air temperature, we prefiltered the data to emphasize 1) the biennial time scale and 2) the decadal time scale and then computed EOFs. The first EOF of both sets of filtered data (not shown) nearly identical to the first EOF based on unfiltered data, and account for 26% (29%) of the variance on biennial (decadal) time scales. In view of the low-frequency behavior of E2 of air temperature, we computed EOFs based on low-pass-filtered data (half power point at five years). The first EOF of the low-pass-filtered data (not shown) resembles the second EOF of the unfiltered data, and accounts for 29% of the variance of the low-pass-filtered data. The correlation coefficient between the time series of E2 (unfiltered) and E1 (low pass) is 0.88. Thus, although the first and second EOFs of unfiltered air temperature are not well separated according to the criterion of North et al. (1982), the sensitivity experiments described above suggest that they are distinct modes of variability.

The similarity of the leading EOFs of the independently measured fields of surface air temperature and SST lends credence to the patterns. The fact that the order of the two leading modes of air temperature and SST is reversed suggests that the orthogonality constraint on the second EOF does not dominate the results. A rotated EOF analysis of air temperature (using the VARIMAX criterion) yields patterns that are very similar to the unrotated modes (not shown).

Recently, Bottomley et al. (1990) have developed a set of "corrections" to the SST data before World War II, designed to account for the effects of changes in measurement technique. The corrections are based on a simple model of air heat transfer from an uninsulated

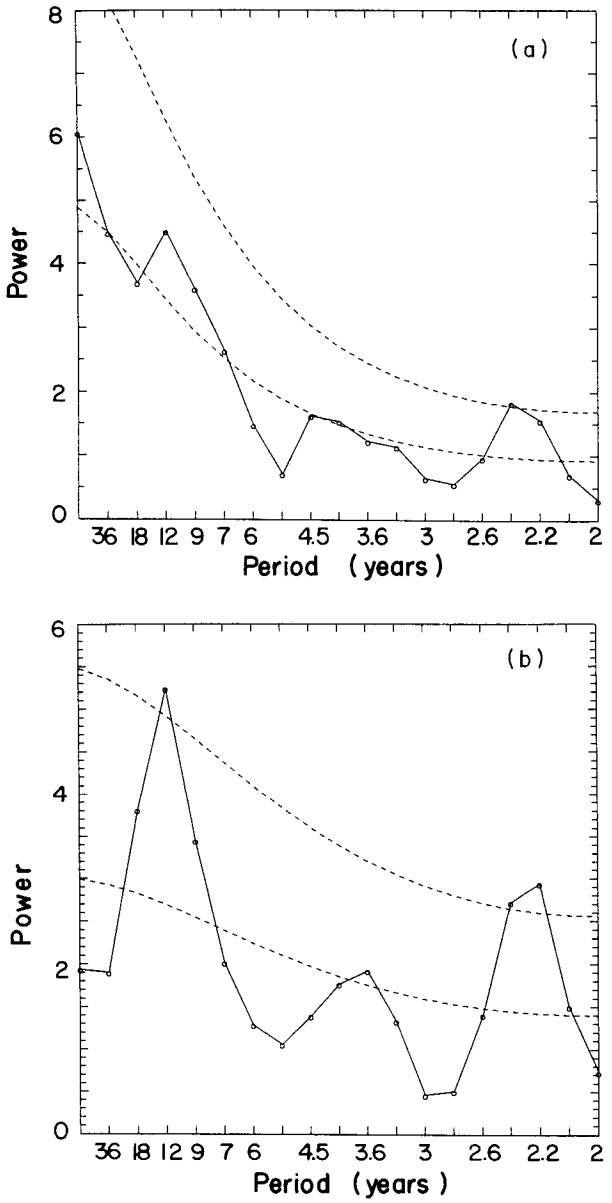

FIG. 3. (a) Power spectrum of EOF 2 of SST. The thin dashed lines represent the background red noise spectrum and its 95% confidence limit. (b) As in (a) but for EOF 1 of air temperature.

bucket subject to the constraint that the difference in the mean annual cycle of SST before and after 1941 is minimized. We performed EOF analysis on these "corrected" SST data. The structure of the biennial/decadal mode is essentially unchanged, but the Gulf Stream mode exhibits maximum amplitude inshore between Cape Hatteras and Nova Scotia, rather than along the Gulf Stream.[2] Whether the Bottomley et al. (1990) corrections are capturing only the artificial trends in the SST data or whether they are also removing part of the climate signal is not adequately resolved at this time. Thus, we are inclined to rely on the consistency between the COADS SST and surface air temperature patterns for demonstration of real climate signals.

b. *Relation of surface temperature variability to the surface atmospheric circulation*

1) DIPOLE PATTERN

How are the dominant modes of variability in surface temperature related to anomalies in the surface atmospheric circulation? Figure 4a shows the patterns of SST and surface wind anomalies regressed upon the time series of E2 SST (a similar picture is obtained if E1 air temperature is used in place of E2 SST). Note that the polarity of E2 SST is opposite from that shown in Fig. 1c, and that the SST pattern has been smoothed in space with a three-point binomial filter. The climatological SST distribution is also shown. The relationship between the surface wind and SST anomalies

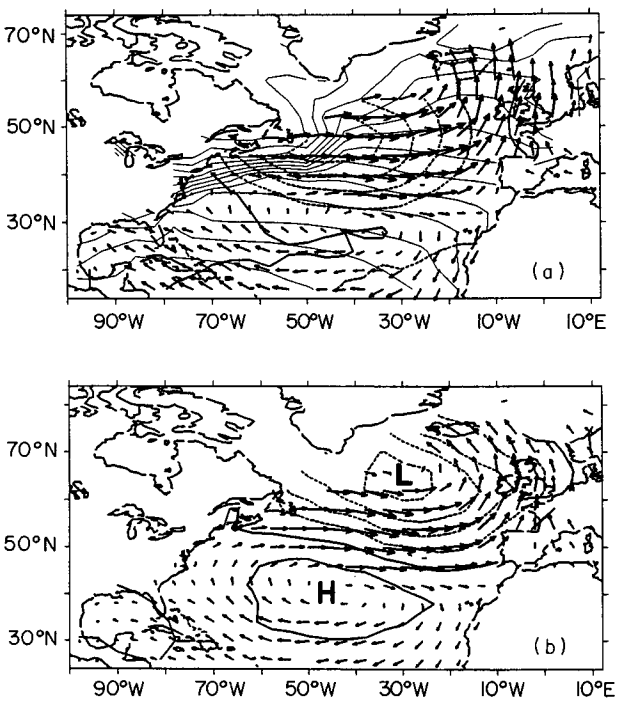

FIG. 4. (a) SST (bold solid and dashed contours) and wind anomalies (arrows) regressed upon the time series of EOF 2 of SST. Also shown is the climatological SST distribution (thin solid contours). Note that EOF 2 of SST has opposite polarity to that shown in Fig. 1c, and has been smoothed in space with a three-point binomial filter. (b) Combined EOF 2 of sea level pressure and zonal wind, based on winter means 1900–89. The meridional wind field was obtained by regressing meridional wind anomalies upon the time series of the combined EOF. This mode explains 15% of the variance in the combined pressure and zonal wind fields.

[2] The Gulf Stream mode (biennial/decadal mode) in the corrected SST dataset accounts for 23% (17%) of the variance.

is primarily local: stronger than normal westerly winds are coincident with cooler than normal temperatures, and southerly (northerly) wind anomalies are associated with warmer (cooler) than normal temperatures. The negative SST anomalies east of Newfoundland are located slightly upstream of the largest wind anomalies where the air–sea temperature differences are largest. The local nature of the wind/temperature relationships suggests that changes in the air–sea fluxes and wind-induced vertical mixing processes contribute to the formation of the SST anomalies. For example, stronger-than-normal winds will cool the ocean mixed layer by enhancing the fluxes of latent and sensible heat from the ocean surface and by accelerating the entrainment of cooler water from below. Ocean modeling experiments by Luksch et al. (1990) and Alexander (1990) confirm this interpretation. A somewhat surprising result is that the wind/temperature relationships are similar on decadal and biennial time scales (not shown).

Is the wind pattern shown in Fig. 4a a preferred mode of variability in the atmosphere? Figure 4b shows the second combined EOF of sea level pressure and zonal wind, based on winter means for 1900–89. This mode accounts for 15% of the variance in the combined fields. The meridional wind pattern was obtained by regressing the meridional wind anomalies upon the time series of the combined EOF. The wind and pressure distributions in Fig. 4b are consistent with the geostrophic relation, lending credence to the patterns. The wind patterns in Figs. 4a and 4b are similar, indicating that E2 SST is coupled to a dominant mode of variability in the atmosphere. The power spectrum of the second combined EOF of pressure and zonal wind, shown in Fig. 5, exhibits peaks at biennial and decadal time scales, similar to those found for E1 air temperature and E2 SST. However, like E2 SST, the decadal peak is not statistically significant. The circulation mode represented by the combined EOF corresponds to the West Atlantic pattern as defined by Wallace and Gutzler (1981), although the northern center of action in the sea level pressure field is centered ~5° east of the corresponding feature in the West Atlantic pattern.[3]

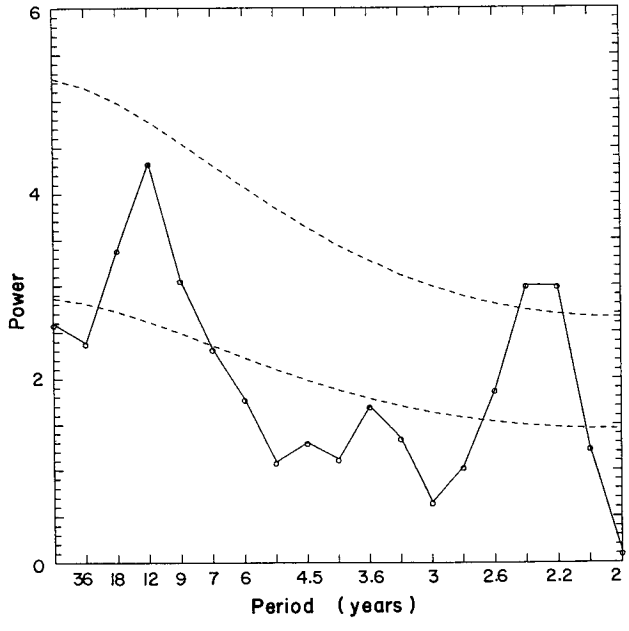

FIG. 5. As in Fig. 3 but for EOF 2 of the combined fields of sea level pressure and zonal wind.

Time series of the various surface parameters to the east of Newfoundland (the center of actions of E1 air temperature and E2 SST) are presented in Fig. 6. These records have been low-pass filtered with a five-point binomial filter. Air temperature and SST were averaged over the region (52°–40°N, 50°–30°W); zonal wind was averaged over the region (48°–38°N, 52°–22°W) and the geostrophic zonal wind was calculated from sea level pressure differences between (40°–32°N, 52°–22°W) and (52°–44°N, 52°–22°W). Note that the air and sea temperatures and winds and pressures were measured independently, so the comparisons provide a means of assessing data quality. All four parameters exhibit variability on quasi-decadal time scales in the area east of Newfoundland; the amplitude of the decadal surface temperature (wind) fluctuations is ~1.5°C (1.5 m s^{-1}). The correlation between the air temperature and SST time series is 0.88, and between the measured and geostrophic wind series, 0.80. The coherence squared between the SST and zonal wind time series (not shown) exceeds the 99% significance level at the decadal period, with a phase lag of 180° between the two parameters.

It is apparent from the time series in Fig. 6 that the time scale of the quasi-decadal fluctuations is longer after ~1940 than before. This is borne out by calculations of the power spectra for the pre- and post-1944 periods. During the period 1900–44, the decadal spectral peak is centered at 9 years whereas during 1945–88, it is centered on 12 years (not shown). Thus, the decadal fluctuations are by no means regular.

2) GULF STREAM PATTERN

The dominant features of the time series of E1 of SST and E2 of air temperature are the cold period of 1900–29 and the warm period 1939–68 (Figs. 1b and 2d). These cold and warm epochs may also be identified on the basis of globally averaged temperatures (cf. Folland et al. 1984) and North Atlantic Basin-averaged temperatures (cf. Bottomley et al. 1990). The surface temperature, wind, and sea level pressure differences between the warm and cold periods are shown

[3] Analysis of 500-mb geopotential height data indicates that the circulation mode shown in Fig. 4b exhibits an equivalent barotropic structure (not shown).

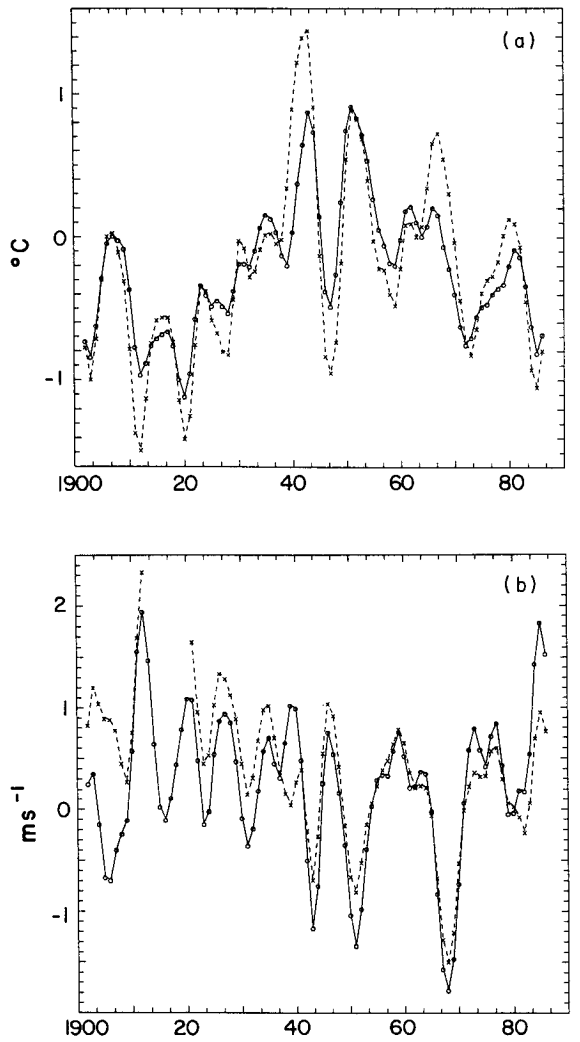

FIG. 6. Time series of winter anomalies east of Newfoundland of (a) SST (solid) and surface air temperature (dashed) and (b) zonal wind (solid) and geostrophic zonal wind calculated from sea level pressure differences (dashed). All curves are smoothed with a five-point binomial filter. See text for definition of indices.

in Fig. 7. A minimum of 20 winters was required for each period average in each grid square. The surface wind and sea level pressure fields (Fig. 7a) are dynamically consistent, with negative pressure anomalies along 40°N and easterly (westerly) wind anomalies to the north (south). The maximum sea level pressure difference is ~3 mb, and the largest wind speed anomaly is ~1.5 m s^{-1}. This circulation pattern resembles the negative phase of the North Atlantic Oscillation (cf. Barnston and Livezey 1987), and represents an overall weakening of the basinwide wind system.[4]

[4] The North Atlantic Oscillation is the dominant mode of variability of the surface atmospheric circulation, accounting for 33% of the variance of the winter sea level pressure field during 1900–89 (not shown).

Similar results were obtained by Parker and Folland (1988) from historical sea level pressure analyses. The SST (Fig. 7b) and air temperature (Fig. 7c) anomaly patterns are grossly similar: both exhibit maximum positive anomalies (~1°C) along the Gulf Stream east of Cape Hatteras, and smaller-amplitude positive anomalies in the eastern ocean. There is some indication of a poleward amplification of the air temperature anomalies, but the data are sparse north of ~55°N. [Stations in Greenland, Iceland, and Scandinavia experienced a ~2°C warming during the 1920s and 1930s (Jones and Kelly 1983).] Although the SST (and to a lesser extent, air temperature) records suffer from discontinuities around World War II (cf. Jones et al. 1986), the similarity between the air and sea tem-

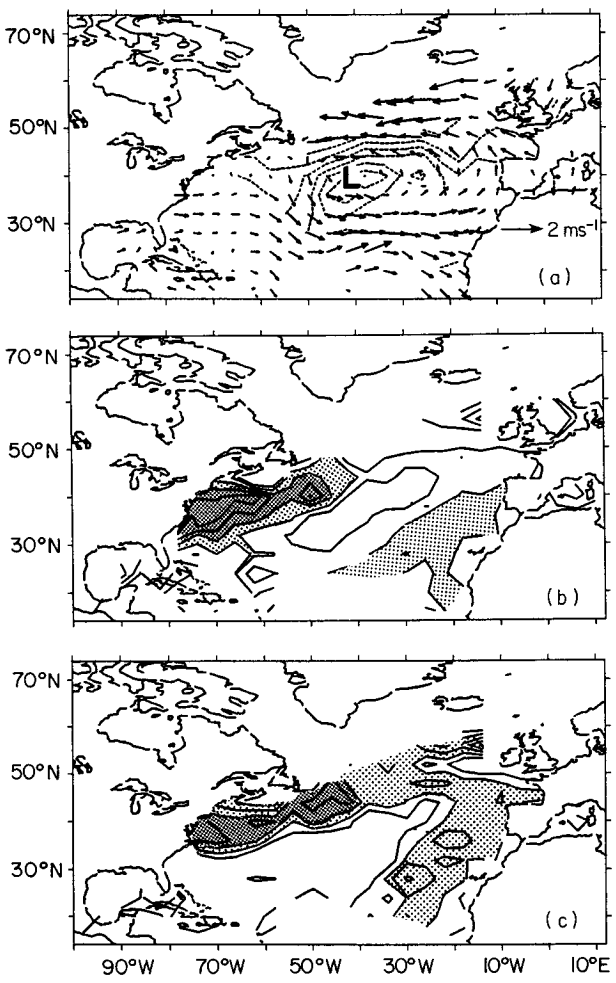

FIG. 7. Difference between the periods 1939–68 and 1900–29 of winter (a) sea level pressure and surface wind, (b) SST, and (c) surface air temperature. In (a) the contour interval is 0.5 mb, with negative contours dashed. The lowest pressure anomaly is −3 mb. Wind scale is indicated in lower right. In (b) light shading indicates values between 0.8°C and 1.0°C; heavy shading indicates values greater than 1.0°C. Contour interval is 0.2°C. In (c) light shading indicates values between 0.6°C and 0.8°C; heavy shading indicates values greater than 0.8°C. Contour interval is 0.2°C.

perature changes lends credence to the patterns. The "corrected" SST dataset of Bottomley et al. (1990) (see section 3a) yields a somewhat different pattern, with maximum warming inshore between Cape Hatteras and Nova Scotia rather than along the Gulf Stream as in the COADS (not shown).

The wind/temperature relationships are different from those associated with the dipole pattern discussed above. While there is some evidence of wind anomalies overlying SST anomalies in the eastern portion of the basin, the largest surface temperature anomalies occur in the west, upstream of the atmospheric circulation anomalies. Whether the temperature anomalies along the Gulf Stream are connected to changes in the strength or position of the current is unknown. However, it is worth noting that a northward shift of the Gulf Stream of only 50 km would be sufficient to produce the observed warming.

To examine the robustness of the patterns, and to test whether the patterns are artifacts of data discontinuities around World War II, we computed the linear least-squares trends during the period 1917–39. The data were first smoothed in time with a three-point binomial filter to enhance the low-frequency signals. The surface wind and sea level pressure fields (Fig. 8a) exhibit a cyclonic circulation trend in the central North Atlantic, similar to the results from the epoch analysis. Over the western North Atlantic, the trend analysis shows easterly wind anomalies, consistent with the pressure field, whereas the epoch analysis shows weak westerly anomalies. The trends in SST (Fig. 8b) and air temperature (Fig. 8c) are similar to the results from epoch analysis, with the largest warming along the Gulf Stream, over the eastern subtropical Atlantic, and near Iceland. The warming along the Gulf Stream is not as continuous, and the warming in the eastern Atlantic not as pronounced, in the trend analysis as in the epoch analysis. As in the epoch analysis, the largest SST trends along the Gulf Stream occur remotely from the wind trends.

The time series of air temperature along the Gulf Stream (44°–36°N, 76°–42°W), and sea level pressure in the central North Atlantic (46°–34°N, 48°–20°W) and at Ponta Delgada, Azores (40°N, 28°W), are shown in Fig. 9. Surface warming along the Gulf Stream occurred during ~1920–50 (amplitude ~2.5°C). Note that the temperatures since the mid-1950s have been relatively constant. The COADS and Ponta Delgada sea level pressure time series show remarkable agreement: both indicate that the warming trend was accompanied by a decrease in the strength of the subtropical high of ~4 mb. The pressure time series give the impression that the downward trend in the atmospheric circulation began ~1905 and lasted until ~1962, although the steepest continuous decline occurred during 1920–40.

Bjerknes (1959) found a similar pattern of warming along the Gulf Stream during the first quarter of this century (he used differences between 1890–97 and 1925–32 to depict the warming trend). The warming was accompanied by a strengthening of the subtropical anticyclone, in contrast to the results of this study. We have attempted to reproduce Bjerknes' (1959) results using data from the COADS. While a warming along the Gulf Stream is hinted at in the COADS, it is much weaker than that depicted in Bjerknes (0.2°C vs 2°C; not shown). The pressure and wind patterns derived from the COADS broadly support Bjerknes' results.

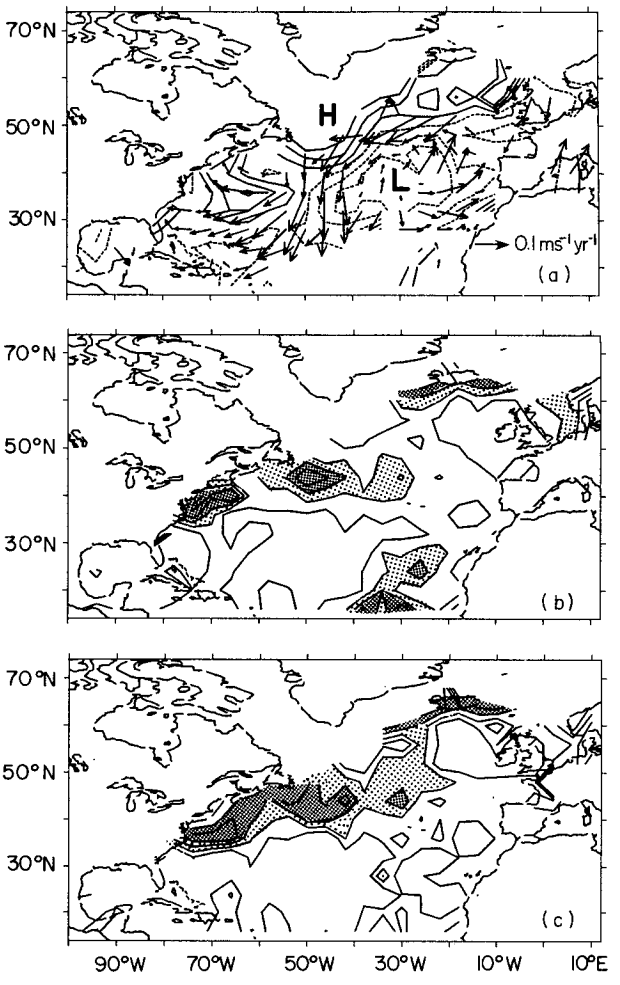

FIG. 8. Linear least-squares trends during 1917–39 of winter (a) sea level pressure and surface wind, (b) SST, and (c) surface air temperature. In (a) contour interval is 0.05 mb per year, with negative contours dashed. The wind scale is given in the lower right. In (b) and (c) the contour interval is 0.02°C yr^{-1}. Light shading indicates values between 0.04°C yr^{-1} and 0.06°C yr^{-1}; heavy shading indicates values greater than 0.06°C yr^{-1}.

4. Discussion

An important mode of variability of the wintertime surface climate over the North Atlantic during this century is characterized by a dipole pattern in SSTs and surface air temperatures, with anomalies of one sign east of Newfoundland, and anomalies of the op-

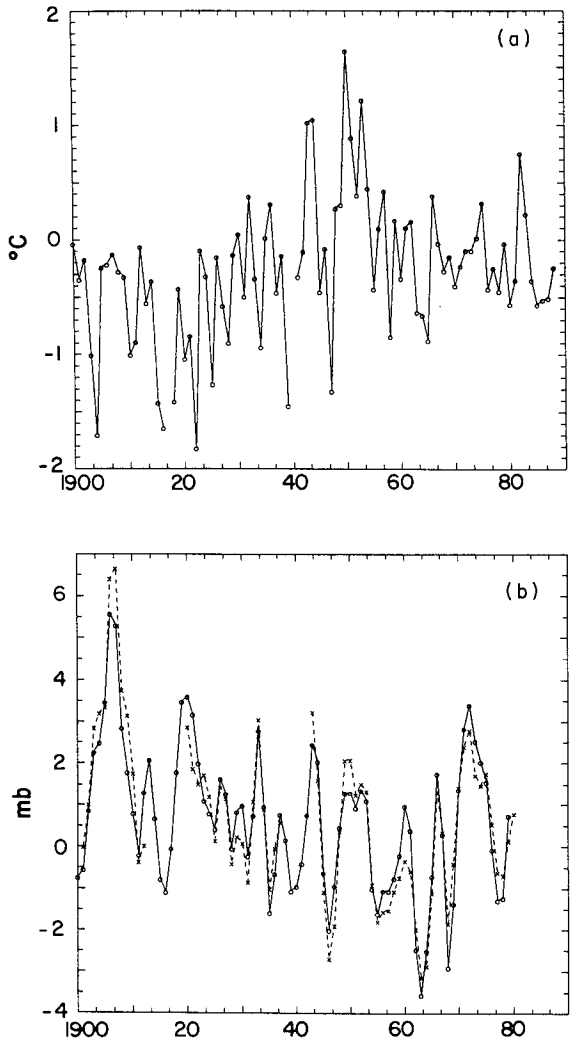

FIG. 9. Time series of winter anomalies of (a) surface air temperature along the Gulf Stream (44°–36°N, 76°–42°W), and (b) sea level pressure in the central North Atlantic (46°–34°N, 48°–20°W) and at Ponta Delgada, Azores (40°N, 28°W). The solid (dotted) curve denotes pressures from Ponta Delgada (COADS). The curves in (b) are smoothed with a three-point binomial filter.

posite polarity off the southeast coast of the United States. This pattern has been noted in the post–World War II data by Wallace et al. (1990), Cayan (1992), and Kushnir (1992). Wind fluctuations occur locally over the regions of large surface temperature anomalies, with stronger-than-normal winds overlying cooler-than-normal SSTs. The atmospheric circulation anomalies resemble the West Atlantic pattern. This mode (both surface temperatures and surface winds) exhibits variability on quasi-biennial and quasi-decadal time scales. The decadal fluctuations are irregular in length, averaging ~9 years before 1945 and ~12 years afterward. There does not appear to be any difference between the wind–SST relationships on the different time scales.

The local nature of the atmosphere–ocean relationships exhibited by the dipole pattern suggests that surface wind anomalies contribute to the formation of SST anomalies by altering the fluxes of latent and sensible heat at the ocean surface and the strength of vertical mixing in the upper ocean. Support for this interpretation is given by the oceanic modeling studies of Alexander (1990) and Luksch et al. (1990).

Further research is needed to understand the origin of the quasi-decadal cycles in the North Atlantic ocean–atmosphere system. One possibility is that 90 years is not long enough to establish the significance of decadal cycles, and those that have occurred may be random in the sense that they are due to internal atmospheric processes. The decadal SST variations could then be interpreted as simply a reflection of low-frequency modulation of the high-frequency (synoptic and monthly) wind forcing. It should be noted that long (100 year) integrations of atmospheric GCMs, subject to fixed SST boundary conditions, exhibit prominent low-frequency (decadal and longer) fluctuations (James and James 1989; Feldstein 1993).

A more inviting possibility is that the quasi-decadal time scale is a property of the coupled ocean–atmosphere system. We note that decadal and longer time scale SST variations along the boundary between the subpolar and subtropical ocean gyres are obtained in ocean GCMs as a result of self-sustained oscillations of the thermohaline circulation (cf. Weaver and Sarachik 1991). In addition, atmospheric GCM experiments indicate that the local atmospheric response to an SST anomaly off Newfoundland is such that weak (strong) winds coincide with high (low) SSTs, reinforcing the original SST anomaly (Palmer and Sun 1985; Lau and Nath 1990). The implication from these studies is that observed midlatitude climate anomalies may result from a positive feedback between the atmosphere and the ocean.

A third possibility is that the decadal atmospheric fluctuations are a response to decadal SST variations outside of the North Atlantic. This scenario is difficult to test due to the lack of lengthy marine records in the other ocean basins. Our preliminary results indicate that for the three most recent decadal oscillations, SSTs in the North Pacific are not coherent with those in the Atlantic. One intriguing link we have found is with sea ice in the Davis Strait–Labrador Sea region. Figure 10a shows the time series of winter sea ice concentration anomalies in the Davis Strait–Labrador Sea region from Agnew (1991), based on data from Walsh and Johnson (1979). The circles denote the winter (December–February) anomaly, plotted in the year in which January occurs. The solid curve shows the data smoothed with a three-point binomial filter. Decadal variability is evident in the sea ice record, with peaks occurring in the winters of 1957/58, 1971/72, and 1983/84. Figure 10b shows the sea ice record superimposed upon the (inverted) time series of the second EOF of winter (November–March) SST (see Fig. 1).

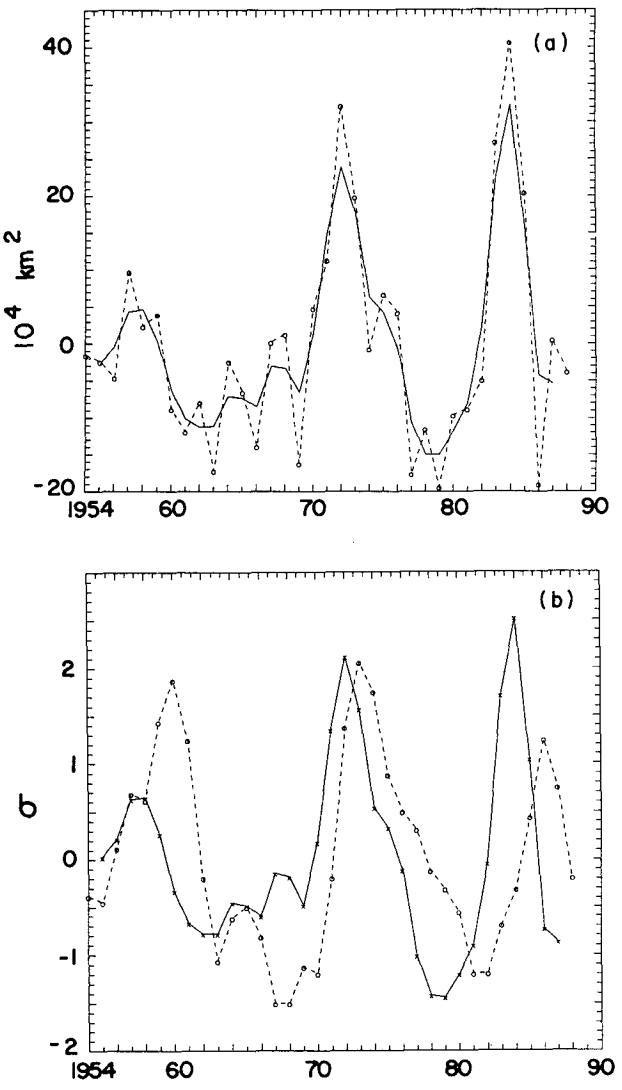

FIG. 10. (a) Time series of winter sea ice area anomalies (10^4 km^2) in the Davis Strait/Labrador Sea region from Agnew (1991), based on data from Walsh and Johnson (1979). The circles denote the winter (December–February) anomaly, plotted in the year in which January occurs. The solid curve shows the data smoothed with a three-point binomial filter. (b) Standardized sea ice anomalies from (a) (solid curve) superimposed upon the standardized time series of EOF 2 of North Atlantic winter (November–March) SST (dashed curve). Note that the SST time series has been inverted. Both the sea ice and SST time series have been smoothed with a three-point binomial filter and detrended by subtracting a least-squares parabola based on the period 1950–88.

Both the sea ice and SST time series have been detrended by subtracting least-squares parabolas based on the period 1950–88, and smoothed with a three-point binomial filter. It may be seen that the maxima in sea ice concentration precede the minima in SST by 1–2 years. The correlation between the two time series is −0.26 at 0 lag; −0.62 when sea ice leads SST by one year; −0.76 when sea ice leads by two years; and −0.62 when sea ice leads by three years. The strong lag correlations indicate that, on the decadal time scale, winters of heavy sea ice in the Labrador Sea precede winters of colder-than-normal SSTs east of Newfoundland. It is plausible that the sea ice anomalies in the Labrador Sea are advected southeastward, resulting in colder-than-normal SSTs east of Newfoundland the following (or second) year. Thus, the quasi-decadal cycle in SSTs east of Newfoundland may result in part from low-frequency Arctic sea ice variations. Mysak et al. (1990) have postulated the existence of an interdecadal Arctic climate cycle, involving runoff and sea ice. Further analysis is needed to elucidate the role of Arctic sea ice in decadal climate variability over the North Atlantic. Diagnosis of the subsurface temperature and salinity variations that accompany the decadal SST anomalies is also needed.

Another dominant mode of variability of the wintertime surface climate over the North Atlantic during this century is associated with the global surface warming trend during the 1920s and 1930s. The patterns of SST and air temperature change between 1900–29 and 1939–68 (or equivalently, the trends during 1917–39) indicate that the warming was concentrated along the Gulf Stream east of Cape Hatteras. Warming also occurred over the Greenland Sea and the eastern subtropical Atlantic. The warming trend was accompanied by a decrease in the strength of the basin-scale atmospheric circulation (negative phase of the North Atlantic Oscillation). In marked contrast to the dipole EOF pattern, the wind changes occurred downstream of the largest SST anomalies. Hence, the gradual surface warming along the Gulf Stream may have been a result of altered ocean currents rather than local wind forcing.

A similar idea has been put forth to explain the cooling trend in the North Atlantic that occurred during the 1950s and 1960s (Levitus 1989; Greatbach et al. 1991; Kushnir 1992). According to a diagnosis of the subsurface temperature and salinity changes by Greatbach et al. (1991), the cooling trend was accompanied by a decrease in the transport of the Gulf Stream. The decreased Gulf Stream transport was in turn traced to bottom pressure torque effects rather than wind changes (Greatbach et al. 1991). It should be noted that the spatial pattern of cooling during the 1950s to 1960s was somewhat different from that of warming during the 1920s and 1930s [see Kushnir (1992) for the pattern of recent cooling].

In a recent coupled atmosphere–ocean general circulation modeling experiment, Manabe and Stouffer (1988) showed that an intensified oceanic thermohaline circulation is associated with surface warming at high latitudes of the North Atlantic, and with an intensification and poleward shift of the Gulf Stream. The model's atmospheric response to an intensified thermohaline circulation is a weakening of the basin-wide wind system, consistent with the reduced baroclinity. It is tempting to speculate that the observed climatic trends over the North Atlantic during the 1920s and 1930s were due to an intensification of the thermohaline circulation. However, we note that SSTs

in the South Atlantic also warmed during this period (cf. Bottomley et al. 1990), contrary to the cooling observed in Manabe and Stouffer's (1988) experiment. Further modeling studies are needed to elucidate the role of the ocean circulation in low-frequency climate variability.

Acknowledgments. We appreciate the thoughtful comments of Drs. Michael Alexander, Peter Lamb, Harry van Loon, Lawrence Mysak, and the two official reviewers. We thank Jon Eischied for providing the Bottomley et al. (1990) dataset and Ludmilla Matrosova for help with the data processing. This work was supported by a grant from NOAA's Climate and Global Change Program.

REFERENCES

Agnew, T., 1991: Simultaneous winter sea ice and atmospheric circulation anomaly patterns. Preprints, *Fifth AMS Conference on Climate Variations,* Amer. Meteor. Soc., Denver, 362–365.

Alexander, M. A., 1990: Simulation of the response of the North Pacific Ocean to the anomalous atmospheric circulation associated with El Niño. *Climate Dyn.,* **5,** 53–65.

Barnett, T. P., 1984: Long-term trends in surface temperature over the oceans. *Mon. Wea. Rev.,* **112,** 303–312.

Barnston, A. G., and R. E. Livezey, 1987: Classification, seasonality, and persistence of low-frequency atmospheric circulation patterns. *Mon. Wea. Rev.,* **115,** 1083–1126.

Bjerknes, J., 1959: *The Recent Warming of the North Atlantic. Rossby Memorial Volume.* B. Bolin, Ed., Rockefeller Inst. Press in assoc. with Oxford University Press, 65–73.

——, 1961: Climatic change as an ocean-atmosphere problem. Proc. Rome Symposium organized by UNESCO and World Meteorological Organization, UNESCO, 297–321.

——, 1962: Synoptic survey of the interaction of the sea and atmosphere in the North Atlantic. Vilhelm Bjerknes Centenary volume, vol. XXIV, *Geofys. Publ.,* No. 3, 115–145.

——, 1964: Atlantic air–sea interaction. *Adv. Geophys.,* **10,** 1–82.

Bottomley, M., C. K. Folland, J. Hsiung, R. E. Newell, and D. E. Parker, 1990: Global Ocean Surface Temperature Atlas.

Broeker, W. S., D. M. Peteet, and D. Rind, 1986: Does the ocean–atmosphere system have more than one stable mode of operation? *Nature,* **315,** 21–16.

Cardone, V. J., J. G. Greenwood, and M. A. Cane, 1990: On trends in historical marine data. *J. Climate,* **3,** 113–127.

Cayan, D. R., 1992: Latent and sensible heat flux anomalies over the northern oceans: Driving the sea surface temperature. *J. Geophys. Res.,* **22,** in press.

Dickson, R. R., J. Meincke, S. A. Malmberg, and A. J. Lee, 1988: The "great salinity anomaly" in the northern North Atlantic 1968–1982. *Prog. Oceanog.,* **20,** 103–151.

Feldstein, S. B., 1993: The relationship between interannual and intraannual variability in atmospheric angular momentum in a GCM with climatological SSTs. *Tellus,* submitted.

Flohn, H., 1986: Singular events and catastrophes now and in climatic history. *Naturwissenschaften,* **73,** 1851–1862.

Folland, C. K., D. E. Parker, and F. E. Kates, 1984: Worldwide marine temperature fluctuations 1856–1981. *Nature,* **310,** 670–673.

Greatbach, R. J., A. F. Fanning, and A. D. Goulding, 1991: A diagnosis of interpentadal circulation changes in the North Atlantic. *J. Geophys. Res.,* **96,** No. C12, 22 009–22 023.

James, I. N., and P. M. James, 1989: Ultra-low-frequency variability in a simple atmospheric circulation model. *Nature,* **342,** 53–55.

Jones, P. D., and P. M. Kelly, 1983: The spatial and temporal characteristics of Northern Hemisphere surface air temperature variations. *J. Climatol.,* **3,** 243–252.

——, T. M. L. Wigley, and P. B. Wright, 1986: Global temperature variations between 1861 and 1984. *Nature,* **332,** 430–434.

Knox, L. J., K. Higuchi, A. Shabbar, and N. E. Sargent, 1988: Secular variation of Northern Hemisphere 50 kPa geopotential height. *J. Climate,* **1,** 500–511.

Kushnir, Y., 1992: Interdecadal variations in North Atlantic sea surface temperature and associated atmospheric conditions. *J. Climate,* in press.

Lau, N. C., and M. J. Nath, 1990: A general circulation model study of the atmospheric response to extratropical SST anomalies observed in 1950–79. *J. Climate,* **3,** 965–989.

Lazier, J. R. N., 1988: Temperature and salinity changes in the deep Labrador Sea 1962–1986. *Deep Sea Res.,* **35,** 1247–1253.

Lehman, S. J., and L. D. Keigwin, 1992: Sudden changes in the North Atlantic circulation during the last deglaciation. *Nature,* **356,** 757–746.

Leith, C. E., 1973: The standard error of time-average estimates of climatic means. *J. Appl. Meteor.,* **12,** 1066–1069.

Levitus, S., 1989: Interpentadal variability of temperature and salinity at intermediate depths of the North Atlantic Ocean, 1970–74 versus 1955–59. *J. Geophys. Res.,* **94,** 6091–6131.

Luksch, U., H. v. Storch, and E. Maier-Reimer, 1990: Modeling North Pacific SST anomalies as a response to anomalous atmospheric forcing. *J. Mar. Syst.,* **1,** 51–60.

Manabe, S., and R. J. Stouffer, 1988: Two stable equilibria of a coupled ocean–atmosphere model. *J. Climate,* **1,** 841–866.

Mysak, L. A., D. K. Manak, and R. F. Marsden, 1990: Sea-ice anomalies in the Greenland and Labrador Seas during 1901–1984 and their relation to an interdecadal Arctic climate cycle. *Climate Dyn.,* **5,** 111–133.

North, G. R., T. L. Bell, R. F. Calahan, and F. J. Moeng, 1982: Sampling errors in the estimation of empirical orthogonal functions. *Mon. Wea. Rev.,* **110,** 699–706.

Palmer, T. N., and Z. Sun, 1985: A modelling and observational study of the relationship between sea surface temperature in the north-west Atlantic and the atmospheric general circulation. *Quart. J. Roy. Meteor. Soc.,* **111,** 947–975.

Paltridge, G., and S. Woodruff, 1981: Changes in global surface temperature from 1880 to 1977 derived from historical records of sea surface temperature. *Mon. Wea. Rev.,* **109,** 2427–2434.

Parker, D. E. and C. K. Folland, 1988: The nature of climatic variability. *Meteorol. Mag.,* **117,** 201–210.

Ramage, C. S., 1987: Secular change in reported surface wind speed over the ocean. *J. Climate Appl. Meteor.,* **26,** 525–529.

Rind, D., D. Peteet, W. Broecher, A. McIntyre, and W. Ruddiman, 1986: The impact of cold North Atlantic sea surface temperatures on climate: Implications for the younger Dryas cooling (11-10 K). *Climate Dyn.,* **1,** 3–33.

Shabbar, A., K. Higuchi, and J. L. Knox, 1990: Regional analysis of Northern Hemisphere 50 kPa geopotential heights from 1946 to 1985. *J. Climate,* **3,** 543–557.

Wallace, J. M., and D. S. Gutzler, 1981: Teleconnections in the geopotential height field during the Northern Hemisphere winter. *Mon. Wea. Rev.,* **109,** 784–812.

——, C. Smith, and Q.-R. Jiang, 1990: Spatial patterns of atmosphere/ocean interaction in the northern winter. *J. Climate,* **3,** 990–998.

Walsh, J. E., and C. M. Johnson, 1979: An analysis of Arctic sea ice fluctuations, 1953–77. *J. Phys. Oceanogr.,* **9,** 580–591.

Weaver, A. J., and E. S. Sarachik, 1991: Evidence for decadal variability in an ocean general circulation model: An advective mechanism. *Atmos.–Ocean,* **29,** 197–231.

Woodruff, S. D., R. J. Slutz, R. L. Jenne, and P. M. Steurer, 1987: A Comprehensive Ocean-Atmosphere Data Set. *Bull. Amer. Meteor. Soc.,* **68,** 521–527.

Wright, P. B., 1986: Problems in the use of ship observations for the study of interdecadal climate change. *Mon. Wea. Rev.,* **114,** 1028–1034.